# Dynamic Fracture Toughness of Cellulose-Fiber-Reinforced Polypropylene: Preliminary Investigation of Microstructural Effects

**CRAIG M. CLEMONS* AND DANIEL F. CAULFIELD**
*USDA Forest Service*
*Forest Products Laboratory*
*One Gifford Pinchot Drive*
*Madison, WI 53705-2398*

**A. JEFFREY GIACOMIN**
*Mechanical Engineering Department and*
*Rheology Research Center*
*University of Wisconsin-Madison*
*309 Mechanical Engineering Bldg.*
*1513 University Ave.*
*Madison, WI 53706-1572*

**ABSTRACT:** In this study, the microstructure of injection-molded polypropylene reinforced with cellulose fiber was investigated. Scanning electron micros-

The use of trade or firm names in this publication is for reader information and does not imply endorsement by the U.S. Department of Agriculture of any product or service.

The Forest Products Laboratory is maintained in cooperation with the University of Wisconsin. This article was written and prepared by U.S. Government employees on official time, and it is therefore in the public domain and not subject to copyright.

This technical paper was originally presented at the 56th Annual Technical Conference of the Society of Plastics Engineers in Atlanta, GA, April 26-30, 1998.

*Author to whom correspondence should be addressed.



0095-2443/99/04 0367-12 $10.00/0

copy of the fracture surfaces and X-ray diffraction were used to investigate fiber orientation. The polypropylene matrix was removed by solvent extraction, and the lengths of the residual fibers were optically determined. Fiber lengths were reduced by one-half when compounded in a high-intensity thermokinetic mixer and then injection molded. At low fiber contents, there is little fiber orientation; at high fiber contents, a layered structure arises. To better understand mechanisms of fracture under impact loading, dynamic fracture analysis was performed based on linear elastic fracture mechanics. Dynamic critical energy release rates and dynamic critical stress intensity factors were deduced from instrumented Charpy impact test measurements. Dynamic fracture toughness increased with cellulose content and with orientation of fibers perpendicular to the crack direction. A preliminary evaluation of a simple model relating the microstructure to the dynamic fracture toughness shows promise, but further work is needed to assess its validity.

**KEY WORDS:** fracture toughness, microstructure, fiber orientation, cellulose fiber.

## INTRODUCTION

**RECENTLY, NATURAL FIBERS** have been used as fillers and reinforcements in low-melting-point thermoplastics. When added to thermoplastics, natural fibers represent low-cost, renewable reinforcements that enhance mechanical properties such as stiffness, strength, and heat deflection under load. Because they have low densities compared with conventional inorganic fillers and reinforcements, these fibers are often used in automotive and packaging applications where the relatively low density of the natural fibers is a major advantage.

The limited fracture toughness of natural-fiber-reinforced thermoplastics at high strain rates can preclude their use in some applications. To understand and ultimately improve the fracture performance of these composites, one must thoroughly understand the composite microstructure and how it affects fracture toughness. Because of methodological difficulties, little work has been performed on characterizing the microstructural parameters such as fiber length and fiber orientation distribution in natural-fiber-reinforced thermoplastics. Even less has been done relating microstructure to composite performance. This research was undertaken to explore the effect of microstructure on the dynamic fracture toughness of cellulose-fiber-reinforced polypropylene.

## EXPERIMENTAL

### Materials

The isotactic polypropylene used in this study was a 12 g/10 min melt flow index homopolymer (Fortilene 1602, Solvay Polymers, Inc., Deer Park, TX). The cellulose fibers were bleached chemical dissolving pulp fibers prepared from southern pine supplied as pressed and dried pulp sheets (Ultranier-J, Rayonier, Jessup, GA).

### Composite Preparation

The polypropylene and cellulose fiber were compounded in a 1-L, high-intensity thermokinetic mixer (K Mixer, Synergistics, Inc., St. Remi de Napierville, QC, Canada). The material was discharged at a set temperature and granulated. Batches of 150 g were processed at a rotor speed of 5000 rpm (rotor tip speed of 32.9 m/s) with discharge temperatures ranging from 180°C to 210°C depending upon the cellulose fiber loading. Resulting batch times ranged from 30 to 60 s. The processing conditions were varied to ensure adequate dispersion and proper discharge.

The compounded material was dried at 105°C for at least 4 h before molding. A 30-metric-ton (33-short-ton) reciprocating screw injection molding machine (Vista Sentry VSX-33; Cincinnati Milacron, Batavia, OH) was used to mold plaques measuring 76 by 127 by 6.4 mm (3 by 5 by 1/4 in). Barrel temperatures did not exceed 200°C and the mold temperature was 40°C. Injection speeds and pressures necessarily varied with the different formulations and material viscosities.

### Dynamic Fracture Tests

Longitudinal and transverse specimens measuring 63.5 by 12.7 by 6.4 mm (2.5 by 1/2 by 1/4 in) were cut from the injection-molded composite plaques (Figure 1). These were then notched with a fly cutter (V notch, 45° angle) to the desired depth, and the crack was sharpened with a razor blade. Specimens were tested at a speed of 1 m/s on an instrumented impact tester (gravity driven) with related software (Dynatup GRC 8250, GRC Instruments, Santa Barbara, CA). A Charpy jig with a 51-mm (2-in) span was used.

Fracture surfaces were sputtered with gold and analyzed on a scanning electron microscope (SEM) (JSM-840, JEOL USA, Inc., Peabody, MA) at a working distance of approximately 25 mm and a voltage of 15 kV.

## Fiber Orientation Determination

For fiber length and orientation determinations, specimens were divided into five equally thick layers: two surface layers, two intermediate layers, and one core layer.

Surface, intermediate, and core layers of each composite were extracted in xylenes for 8 h. The resulting polypropylene-free cellulose fiber mats were analyzed using a diffractometer with related software (HI-STARR detector with GADDS 3.310 software, Siemens Energy and Automation, Madison, WI). Each extracted sample was irradiated with Cu K$\alpha$ X-rays for 60 s at 40 kV and 20 mA using a 0.8-mm collimator. The resulting intensities from the [200] plane of the cellulose crystal structure at $2\theta = 22.9°$ were used to determine the following orientation parameters [1]:

$$f_p = 2\langle \cos^2 \chi \rangle - 1 \tag{1}$$

$$\langle \cos^2 \chi \rangle = \frac{\Sigma N(\chi_i) \cos^2 \chi_i}{\Sigma N(\chi_i)} \tag{2}$$

where $\chi$ is the azimuthal angle and $N(\chi)$ is the intensity at a given $\chi$. Because there is a distribution of crystalline cellulose orientation around the fiber axis, values of $|f_p|$ were artificially low. Instead of attempting to quantitatively deconvolute the fiber orientation and cellulose crystal distributions, an approximate method was used. The orientation parameter $f_p$ was normalized using an average orientation parameter of solid loblolly pine (*Pinus taeda*), which was selected to represent a perfectly aligned composite.

## Fiber Length Determination

Approximately 0.4 mg of residual fibers from the extracted samples were dispersed in 1 L of deionized water. Fiber lengths were then measured by an optical method (Kajaani FS-100, Kajaani GmbH Automation, Norcross, GA). The cellulose fibers were forced through a capillary pipette located between a light source and a photocell. The shadow falling on the diodes in the detector was used to calculate fiber length. At least 2000 fibers were measured for each sample. Average fiber lengths were calculated using

$$L_n = \frac{\Sigma n_i l_i}{\Sigma n_i} \tag{3}$$

$$L_w = \frac{\Sigma n_i l_i^2}{\Sigma n_i l_i} \tag{4}$$

where $L_n$ and $L_w$ are the number and weight average fiber lengths, respectively, and $n$ is the number of fibers of length $l$ in the $i$th range. An average fiber diameter $D$ of 20 μm was determined by examining many scanning electron micrographs and was used in determining aspect ratios.

## RESULTS AND DISCUSSION

### Composite Microstructure

The SEM micrographs of the high cellulose fiber content composites revealed a layered structure (Figure 1) resembling that of injection-molded glass-fiber-reinforced thermoplastics [1]. As the melt enters the mold, the sudden increase in channel dimensions causes deceleration along the flow direction and hence a compressive force. This compression aligns the fibers transversely to the melt flow direction. Fibers near the surface of the plaques orient parallel to the filling through elongational flow at the flow front. Rose calls this the "fountain effect" [2]. Due to rapid injection speeds, flow in the core region approaches plug flow and the transverse fiber alignment created at the gate is maintained. This morphology was most obvious in the composite samples with higher fiber contents. Figures 2 and 3 show different

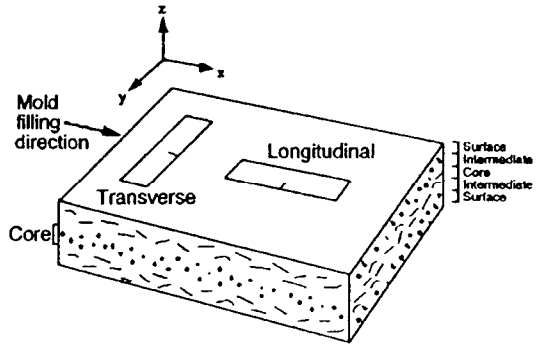


**FIGURE 1.** Fiber alignment with respect to melt flow direction for high fiber content composites.


**FIGURE 2.** Fracture surface of 40% cellulose fiber composite near outer surface of a longitudinal specimen. Fiber orientation out of *y-z* plane (Figure 1).

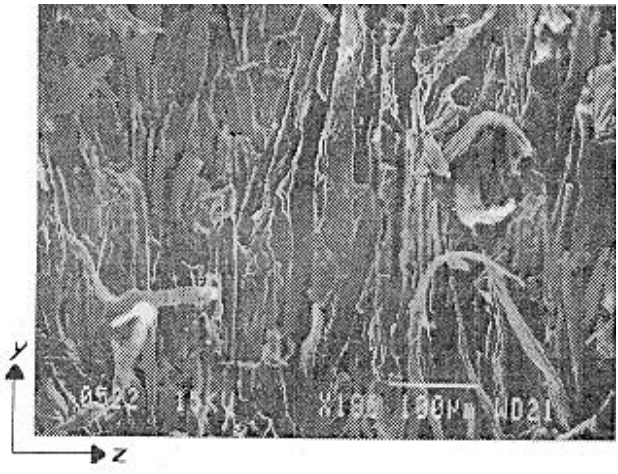


**FIGURE 3.** Fracture surface of 40% cellulose fiber composite at the core of a longitudinal specimen. Fiber orientation in they direction of the y-z plane (Figure 1).

regions of a fracture surface of a longitudinal specimen exhibiting this layered structure. Identifying precise transitions between core and surface morphologies is difficult so each sample was divided into five equally thick layers (one core, two surface, and two intermediate layers) for further microstructural analyses (Figure 1).

Figure 4 summarizes the orientation parameters $f_p$ from the X-ray analysis. The $f_p$ function yields a positive value for orientation in the flow direction, a negative value for orientation across the flow direction, and nearly zero for random orientation. The trends shown in Figure 4 confirm observations from the SEM work. The preferred fiber orientation is perpendicular to the flow direction in the core layer and parallel to the flow direction in the surface layer. This layered structure decreases with decreasing cellulose fiber content, and nearly random orientation is found at low cellulose fiber contents.

Number average aspect ratios $L_n/D$ and $L_n/L_w$ ratios are summarized in Table 1. Because of fiber breakage, average aspect ratios were halved during compounding and injection molding. The fiber lengths nearly matched for composites of differing fiber content, despite differences in viscosities and processing conditions during compounding and molding.

## Fracture Toughness Tests and Modeling

Linear elastic fracture analysis [3] was used to evaluate dynamic fracture toughness of whole Charpy specimens before sectioning. For

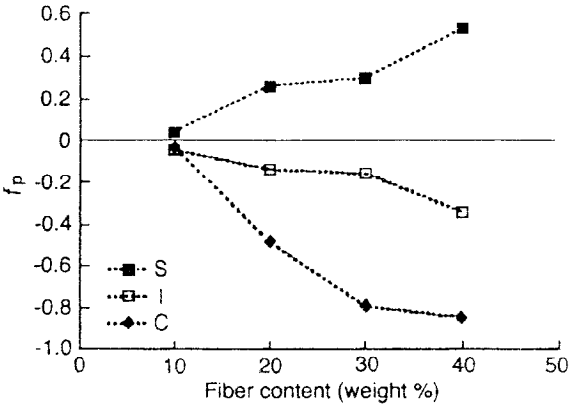


**FIGURE 4.** Fiber orientation parameter ($f_p$) determination results (S, surface. I, intermediate; C, core).

*Table 1. Summary of microstructural data for cellulose fiber (CF) and cellulose fiber-polypropylene composites.*

| CF (wt %) | Layer[a] | Volume Fraction, $V_f$ | Fiber Orientation Parameter,[b] $f_p$ | Effective Fiber Orientation Parameter, $f_{p,eff}$ | Aspect Ratio, $L_n/D$ | $L_n/L_w$ | Reinforcement Effectiveness Factor[c] $R_L$ | $R_T$ |
|---|---|---|---|---|---|---|---|---|
| 100 | NA[d] | NA | NA | Fiber NA | 51.0 | 0.38 | NA | NA |
| | | | | Composites | | | | |
| 10 | C | 0.067 | -0.03 | 0.43 | 23.0 | 0.29 | | |
| | I | 0.067 | -0.04 | 0.40 | 23.0 | 0.30 | 0.19 | 0.23 |
| | S | 0.059 | 0.04 | 0.60 | 21.5 | 0.28 | | |
| 20 | C | 0.145 | -0.49 | 0.05 | 21.5 | 0.29 | | |
| | I | 0.145 | -0.14 | 0.22 | 22.5 | 0.31 | 0.31 | 0.68 |
| | S | 0.140 | 0.25 | 0.89 | 23.0 | 0.34 | | |
| 30 | C | 0.240 | -0.80 | 0.05 | 24.0 | 0.29 | | |
| | I | 0.210 | -0.17 | 0.19 | 23.5 | 0.30 | 0.45 | 1.07 |
| | S | 0.208 | 0.29 | 0.90 | 23.0 | 0.31 | | |
| 40 | C | 0.339 | -0.85 | 0.06 | 24.5 | 0.29 | | |
| | I | 0.316 | -0.35 | 007 | 24.0 | 0.29 | 0.60 | 1.66 |
| | S | 0.311 | 0.52 | 0.95 | 23.0 | 0.32 | | |

[a]C, center layer; I, intermediate layer; S, surface layer.
[b]Orientation parameters calculated using flow direction as reference.
[c]For calculation of *R* values, $f_{p,eff}$ was used for transverse specimens ($R_T$), 1 - $f_{p,eff}$ for longitudinal specimens ($R_L$). *R* values refer to the summation of the C, I, and S layers and were calculated using Equation (7).
[d]NA, not applicable.

evaluation of dynamic critical stress intensity factors $K_c$, the following equation was used:

$$\sigma Y = K_c (a)^{-1/2} \tag{5}$$

where $\sigma$ is the maximum gross bending stress, $Y$ is a calibration factor, and a is crack length. Inertial energy effects were previously found negligible for our experimental setup [4]. Specimens with various crack depths were tested, and fracture toughness parameters were determined from the slopes of $\sigma Y$ plotted against $(a)^{-1/2}$. The assumption of linear elastic behavior was based on the linearity of stress vs. strain curves and $\sigma Y$ vs. $(a)^{-1/2}$ curves. At least 10 specimens were used for each $K_c$ determination. Values for $Y$ have been determined elsewhere [5].

Figure 5 summarizes the critical stress intensity results. The increase in fracture toughness with fiber content is consistent with re-

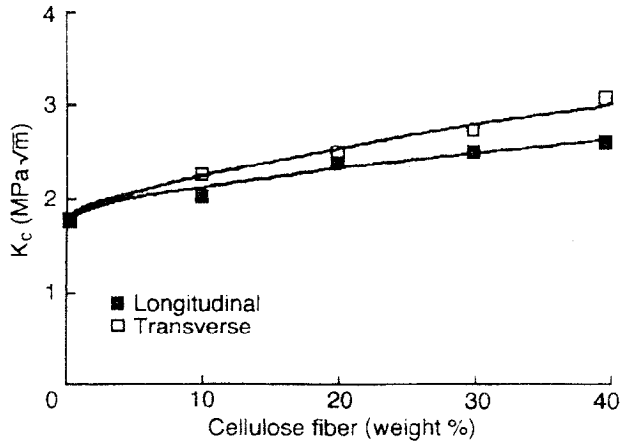


**FIGURE 5.** Effect of fiber content on dynamic critical stress intensity factors (Kc). Longitudinal and transverse specimens

ports of other reinforcing fibers in polypropylene [1]. Interestingly, in this system, the increases in toughness are accompanied by increases in both strength and modulus.

Little difference in fracture toughness was seen between transverse and longitudinal specimens. This small difference can be attributed to the greater overall fiber alignment across the crack path in the transverse specimens (Figures 1 and 4).

We then used Friedrich's microstructural efficiency model to relate microstructure to fracture performance of various short-fiber composites [1,6,7]:

$$\frac{K_{c,C}}{K_{c,M}} = a^* + nR \tag{6}$$

where $K_c$,$C$ is the fracture toughness of the composite and $K_{c,M}$ is the matrix toughness. The $a^*$ is the matrix toughness correction factor, which reflects changes in the fracture toughness of the matrix as a result of the fiber presence (for example, transcrystallinity at fiber-matrix interfaces). The $n$ is the energy absorption ratio and reflects the increase in toughness directly attributed to the fibers (fiber debonding, pull-out, or fracture). $R$ is the dimensionless reinforcement effectiveness factor:

$$R = \Sigma_i T_{rel,i} V_{f,i} F_{L,i} F_{O,i} \tag{7}$$

where $T_{rel,i}$ is the thickness of the $i$th layer divided by the overall thickness, $V_{f,i}$ is the volume fraction of the $i$th layer, and $F_{L,i}$ and $F_{O,i}$ are the fiber length and orientation efficiency factors. In this study, the microstructural parameters are summed for the surface, intermediate, and core layers.

Although the thickness and volume fractions are easily represented, efficiency factors for the length and orientation distributions, $F_{L,i}$ and $F_{O,i}$, are more difficult. As a first-order approximation of the aspect ratio distribution, Karger-Kocsis and Friedrich [6] proposed using the product of maximum aspect ratio and a representation of the width of the distribution curve:

$$F_O = \frac{(L/D)_{max}(L/D)_n}{(L/D)_w} \tag{8}$$

where $(L/D)_{max}$ is the peak aspect ratio and $(L/D)_n$ and $(L/D)_w$ are the number and weight average aspect ratios.

The effective orientation parameter, $f_{p,eff,i}$, is

$$f_{p,eff} = \alpha[1 + \tanh(\beta f_p)] \tag{9}$$

where $f_p$ is the orientation factor determined by Equations (1) and (2), $a = 0.5$, and $1 < \beta < 5$ for $0 \leq |f_P| \leq 1$ [6].

Table 1 summarizes the microstructural data and calculated reinforcing effectiveness parameters. The reinforcing effectiveness fac-

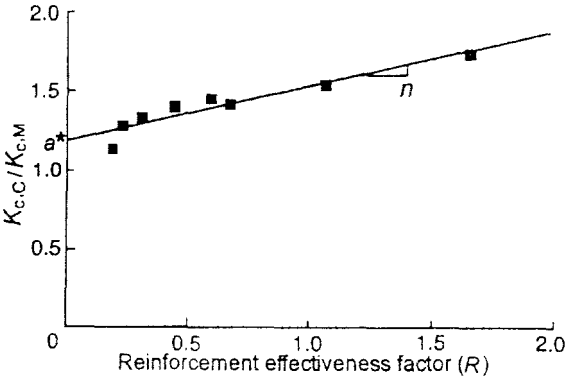


**FIGURE 6.** Effect of microstructure on dynamic fracture toughness. $K_{c,C}/K_{c,M}$ is the ratio of fracture toughness of the composite to that of the matrix ($a^*$ is the matrix toughness correction factor, $n$ is the energy absorption ratio).

tors were determined for each composite according to Equation (7) and were plotted against a normalized critical stress intensity (Figure 6). An approximate linear correlation was found, with little scatter, despite the dynamic nature of the test. Values of 1.12 and 0.27 were found for $a^*$ and $n$, respectively. When $a^*$ exceeds 1, there is an improvement of the matrix toughness with fiber addition. A positive value of $n$ indicates an improvement in fracture toughness of the composite directly attributable to the addition of cellulose fiber.

## CONCLUSION

1. Number average aspect ratios $L_n/D$ were reduced by one-half when compounded in a high intensity thermokinetic mixer and then injection molded.
2. At low fiber contents, there was little fiber orientation; at high fiber contents, a layered structure arose.
3. Dynamic fracture toughness increased with cellulose content and with orientation of fibers perpendicular to the crack direction.
4. A preliminary evaluation of Friedrich's microstructural efficiency model relating microstructure to dynamic fracture toughness showed promise.

Although good correlation between the fracture toughness and microstructure was found, work to date has not tested several aspects of the model. For example, little change was seen in fiber length distribution, and a considerably larger $R$ value range is desired. Changing key processing parameters would alter composite morphology and, ultimately, fracture toughness. An investigation of this type would demonstrate how fracture toughness can be controlled through processing. Future work will address this.

## ACKNOWLEDGMENTS

The authors gratefully acknowledge Solvay Polymers, Inc. (Deer Park, TX) and Rayonier, Inc. (Jessup, GA) for supplying the polypropylene and cellulose fiber. The authors also thank the Chemical Engineering Department of the University of Wisconsin-Madison for the use of their X-ray equipment and the National Center for Agricultural Utilization Research (Peoria, IL) for use of their impact testing equipment.

## REFERENCES

1. Spahr, D. E., K. Friedrich, J. M. Schultz, and R. S. Bailey. 1990. *Journal of Materials Science,* 25:4427–4439.
2. Rose, W. 1961. *Nature,* 191:242.
3. Plati, E. and J. G. Williams. 1975. *Polymer Engineering and Science,* 15(6): 470–477.
4. Clemons, C. M., A. J. Giacomin, and J. A. Koutsky. 1997. *Polymer Engineering and Science,* 37(6):1012–1018.
5. Friedrich, K. (ed.). 1989. *Application of Fracture Mechanics to Composite Materials.* New York, NY: Elsevier Science Publishers B.V.
6. Karger-Kocsis, J. and K. Friedrich. 1988. *Composites Science and Technology,* 32:293–325.
7. Friedrich, K. 1985. *Composites Science and Technology,* 22:43–74.

**VOLUME 31 NUMBER 4**
**OCTOBER 1999**
ISSN 0095-2443

# JOURNAL OF

# ELASTOMERS

# AND PLASTICS

TECHNOMIC
PUBLISHING CO., INC.